Analytical Methods

PAPER

View Article Online
View Journal | View Issue

Cite this: *Anal. Methods*, 2014, **6**, 2371

Simultaneous determination of hydroquinone and catechol in compost bioremediation using a tyrosinase biosensor and artificial neural networks†

Zhou Yaoyu,[ab] Tang Lin,*[ab] Zeng Guangming,*[ab] Zhang Yi,[ab] Li Zhen,[c] Liu Yuanyuan,[ab] Chen Jun,[ab] Yang Guide,[ab] Zhou Lu[ab] and Zhang Sheng[ab]

A biosensor based on tyrosinase immobilized with ordered mesoporous carbon–Au (OMC–Au), L-lysine membrane and Au nanoparticles (tyrosinase/OMC–Au/L-lysine/Au) was combined with artificial neural networks (ANNs) for the simultaneous determination of catechol (CC) and hydroquinone (HQ) in compost bioremediation of municipal solid waste. The good performance of biosensor provided the potential applicability for the simultaneous identification and quantification of catechol and hydroquinone in real samples, and the combination with ANNs offered a good chemometric tool for data analysis in respect to the dynamic, nonlinear, and uncertain characteristics of the complex composting system. Good prediction ability was attained after the ANNs model optimization, and the direct detection range for catechol and hydroquinone were directly analyzed by the ANNs model and varied between 1.0×10^{-7} and 1.1×10^{-4} M, significantly extended compared to the linear model (4.0×10^{-7} to 8.0×10^{-5} M). Finally, the performance of the ANNs model was compared with the linear regression model. The results demonstrate that the prediction results by the ANNs model are more precise than those by the linear regression, and the latter was far from accurate at high levels of catechol and hydroquinone beyond the linear range. All the results show that the combination of the biosensor and ANNs is a rapid and sensitive method in the quantitative study of composting system.

Received 7th November 2013
Accepted 20th January 2014

DOI: 10.1039/c3ay41976b

www.rsc.org/methods

Introduction

Phenolic compounds are widely distributed as environmental pollutants because many of them are resistant to biotic and abiotic degradation. They are mostly derived from various agricultural and industrial activities, including waste discharge from wood preservatives, coking, textiles, plastics, dyes, paper, herbicides industries and the partial degradation of phenoxy contaminants in remediation processes.[1,2] The toxicity of phenols generated from bioremediation processes, such as composting, can bring on undesirable ecological effects and seriously reduce removal efficiencies.[3] Catechol (CC) and hydroquinone (HQ) are two isomers of phenolic compounds which are harmful to human health and ecological environment. During the application of composting technology in disposal of municipal solid waste, CC and HQ are generally direct pollutants or by-products of the aromatic pollutant.[4] Therefore, detection and quantification of the toxicity of these phenolic compounds from compost bioremediation of municipal solid waste is a critical issue. Up to now, a great number of analytical methods have been established to determine dihydroxybenzene isomers in compost systems. On the one hand, there are techniques such as high-performance liquid chromatography (HPLC),[5] spectrophotometry[6] and gas chromatography,[7] which allow individual identification of phenols, but these procedures usually require specific equipment, laboratory conditions, and are not suitable for on-site analyses. On the other hand, electrochemical methods are applied to detect the hydroquinone, catechol, phenol, resorcinol, cresol. These methods have the advantages of fast response, cheap instrument, low cost, simple operation, timesaving, but the key point lies in improving the sensitivity, selectivity and the potential applicability for the quantification of phenols in real samples. In an attempt to overcome the deficiencies of these analytical methods, the applications of enzyme sensors to specific pollutant detection have been increasingly reported to exhibit superior sensitivity, stability, reusability, selectivity, and portability.[8] The biosensor provided the potential to quantify the pollutant levels in real environmental samples. The operation efficiency of compost systems will be much improved if enzyme sensors are applied in pollutant detection.

[a]*College of Environmental Science and Engineering, Hunan University, Changsha, 410082, China. E-mail: tanglin@hnu.edu.cn; zgming@hnu.edu.cn; Fax: +86-731-88822778; Tel: +86-731-88822778*

[b]*Key Laboratory of Environmental Biology and Pollution Control, Hunan University, Ministry of Education, Changsha 410082, China*

[c]*The Institute of Packaging and Materials Engineering of Hunan University of Technology, Zhuzhou 412007, China*

† Electronic supplementary information (ESI) available. See DOI: 10.1039/c3ay41976b

In our previous work, a tyrosinase biosensor was developed for linear calibration and simultaneous determination of hydroquinone and catechol.[9] The biosensor was evaluated by differential pulse voltammetry (DPV) measurements, which is used to make electrochemical measurements, and the DPV peak currents increased linearly with concentration over the range of 4.0×10^{-7} to 8.0×10^{-5} M, the detection limits of HQ and CC were 5×10^{-8} and 2.5×10^{-8} M ($S/N = 3$), respectively. The sensitivities in the linear calibration regions for low concentrations showed the following order: 0.4511 A/M (catechol, $n = 4$) > 0.338 A/M (hydroquinone, $n = 13$). The electrode showed a rapid and sensitive bioelectrocatalytic response of 65 and 89 s after addition of catechol and hydroquinone, respectively. Using the differential pulse voltammetry (DPV), the wide peak separation and low peak potential ensured the avoidance of interferences, making this biosensor a potential device for real sample applications. However, the detection procedures are still susceptible to the complex samples containing heterogeneous organic components and certain functional groups, such as phenolic OH and carboxyl, especially in compost system in which a variety of organic compounds coexist, owing to both the redox and sorption of the interfering matrix constituents on the electrode surface.[8] As a result, an unstable baseline or even the overlapped differential pulse voltammetry signal will be obtained with a carbon electrode when it was applied to large quantities of compost samples. Although the data generated by simultaneous determination of phenol compounds from compost bioremediation can be analyzed using the linear regression model, nonlinearities and uncertainties also occur in the process as mentioned above, which restrict the biosensor in practical applications. Thus, the quantification capability of the linear model will be limited by the dynamic, nonlinear, and uncertain characteristics of the complex composting system, and will give erroneous results if the linear range is exceeded. Artificial neural networks (ANN) are computational models inspired by animal central nervous systems (in particular the brain) that are capable of machine learning and pattern recognition. They are usually presented as systems of interconnected "neurons" that can compute values from inputs by feeding information through the network. They have found extensive utilization in solving many complex real-world problems. ANNs could be deemed as advanced signal processing variants allowing the interpretation, modelling and calibration of complex analytical signals for they can process very nonlinear and complex problems even if the data are imprecise and noisy.[8,10,11] The combination of the tyrosinase biosensor with ANNs modelling may represent an alternative to classical methods. This approach has already been introduced towards the analysis of phenols. For example, the group of Xavier Cetó and Francisco Céspedes has used this method to manage the sensor signal, and established electronic tongue and Bio-Electronic Tongue (BioET) based on voltammograms correlated to phenol contents in wines.[12–16] In addition, the Tang group has used this method to handle the biosensor signal, processing the amperometric signals correlated to enzyme activities or phenol contents in compost systems.[8,26]

In this work, the application of ANN technique for evaluation of the DPV signals of multi-component analysis generated by the tyrosinase biosensor for the simultaneous determination of CC and HQ in compost extract samples was explored, which has not been reported. This method combining the advantages of both parts, calibrated the complex overlapping analytical signals and imprecise data from composting samples. The aim of the study is to extend the limited measuring range of the biosensor to a useful and wider working band. This assay provides the potential applicability of the biosensor for the quantification of CC and HQ in compost system, and the development of fast and inexpensive on-line monitoring systems in municipal solid waste compost bioremediation.

Experimental

Apparatus and reagents

Cyclic voltammetric (CV) measurement and differential pulse voltammetry (DPV) measurement were carried out on CHI660B electrochemistry system (Chenhua Instrument, Shanghai, China). Model PHSJ-3F laboratory pH meter (Leici Instrument, Shanghai, China) was used to test the pH value. A Sigma 4K15 laboratory centrifuge, a vacuum freezing dryer and a mechanical vibrator were used in the assay. The three-electrode system used in this work consisted of a tyrosinase/ordered mesoporous carbon–Au (OMC–Au)/L-lysine/Au/glassy carbon electrode (GCE) as working electrode, a saturated calomel electrode (SCE) as reference electrode and a Pt foil auxiliary electrode. All the work was conducted at room temperature (25 °C) unless otherwise mentioned.

Tyrosinase (EC 1.14.18.1, from mushroom as lyophilized powder), catechol and hydroquinone were purchased from Sigma-Aldrich (USA). Tetraethoxysilane (TEOS), L-lysine, gold(III) chloride trihydrate ($HAuCl_4 \cdot 4H_2O$, 99.9%) and all other chemicals were of analytical grade and used as received. Phosphate buffer solutions (1/15 M PBS) with different pH 6.98 were prepared by mixing the stock solutions of KH_2PO_4 and $Na_2HPO_4 \cdot 12H_2O$. All solutions were prepared with double-distilled water. The synthesis of OMCs-Au nanoparticles and the immobilization of tyrosinase on the surface of nanoparticles were achieved according to the procedure introduced by Tang *et al.*[9]

Procedures

The preparation of tyrosinase/OMC–Au/L-lysine/Au/GCE and the measurements of CC and HQ were carried out as described in our previous work.[9] Briefly, the Au nanoparticles (AuNPs) and L-lysine were immobilized on a glassy carbon electrode by electrochemical method. OMC–Au/L-lysine/Au/GCE was prepared by casting 5.0 μL of the OMC–Au suspension onto the surface of the L-lysine/Au/GCE, Finally, tyrosinase was immobilized on the electrode surface, as presented in Scheme S1.† AuNPs modified glassy carbon electrode (GCE) due to their high effective surface area, nano-scaled dimension effects, and most importantly, binding affinity with L-lysine. In addition, L-lysine provided amino and became the cross-linking agent between AuNPs film and OMC–Au film, and OMC–Au could not only unite with

L-lysine, but also combined with tyrosinase. This makes the enzyme more fixed on the biosensor, accelerates the electron transfer from the enzyme-catalysed redox reaction to electrode surface, and extends its functional life as well.[9] Under the optimized condition, 10 mL compost extract samples containing different concentrations of CC and HQ were added into an electrochemical cell, and then the three-electrode system was installed on it. The DPV was recorded from +0.6 to −0.2 V with pulse amplitude of 0.05 V, pulse width of 0.05 s, and pulse period of 0.2 s. The CV was performed between −0.6 and +0.8 V at scan rate of 50 $mV \cdot s^{-1}$, sample interval of 0.0001 V and quiet time of 2 s.

Preparation of compost extracts

The biosensor simultaneous determination of the CC and HQ concentration was applied in compost bioremediation. The composting process has been introduced previously.[17] The components of compost were soil, straw, restaurant leftover, and bran, and the water ratio was 51%. The soil was collected from 100 cm underground on the unfrequented hillside of Yuelu Mountain (Changsha, China), from which large organic scraps were removed. Then aerobic compost was managed 40 days under the condition of 30 °C temperature and 0.033 $m^3\ h^{-1}$ ventilation. 10 g of compost sample was placed in a flask and 200 mL water was added in. The suspension was agitated on a mechanical vibrator at 200 rpm for 2 h. The supernatant was centrifuged at 10 000 rpm for 5 min, and then filtered to get the filtrate as the compost extract. All the work was done at room temperature unless otherwise mentioned. The dosage of CC and HQ into each compost extract was controlled using certain volumes of CC and HQ stock solutions.

Data processing

Chemometric processing was done by specific routines in MATLAB 7.0 (Math Works, Natick, MA) written by the authors, using Neural Network Toolboxes to develop the ANN models. Sigma Plot 12.0 (Systat Software Inc, California, USA) was used for graphic representations of data and results.

The measured data of a total set of 38 samples using the biosensor were divided into three datasets. Twenty-two samples for the training set were used to build the proper modeling of the response, 8 samples randomly distributed for the testing set were used to estimate the modeling performances, and another 8 extract samples were used to validate the ANN model application. The biosensor DPV responses of compost samples with corresponding CC and HQ concentrations were analyzed using a feed-forward back propagation (BP-ANN). This artificial neural network model for variable selection aims to find an optimal set of inputs that can quickly and successfully classify or predict the desired outputs. It was a feed-forward network combining a back propagation algorithm which was used to train the network according to a learning rule.[18] For each sample, a complete DPV was recorded for forming the array and data. In order to reduce the high dimensionality of the recorded signals, to prevent larger numbers from overriding smaller ones, and to prevent premature saturation of hidden nodes, which impedes the learning process, a pre-processing stage was required. There is no one standard procedure for normalizing inputs and outputs.[19] However, it is recommended that the data be normalized between slightly offset values such as 0.1–0.9 and to avoid saturation of the sigmoid function leading to slow or no learning.[20,21] For this, the input values of both the training and the test subsets were kept in interval [0.1,0.9] corresponding to the range of the normalized function:

$$X_i = 0.1 + 0.8\left(\frac{Z_i - Z_{i\,min}}{Z_{i\,max} - Z_{i\,min}}\right) \quad (1)$$

where X_i is the normalized value of input variable, Z_i is the original value, and $Z_{i\ max}$, $Z_{i\ min}$ are the maximum and minimum original values of primitive data, respectively. After simulation of the networks, the estimated results were reconverted by inverse function of eqn (1) to be compared with the target values.

For complete assessment of model performances, the root mean square error (RMSE) was used, which was calculated between expected and predicted concentration values for each sample (i) and for each of the two analytes (j) considered:

$$\mathrm{RMSE} = \sqrt{\frac{\sum_{ij}\left(Z_{ij} - \overline{Z}_{ij}\right)^2}{3n-1}} \quad (2)$$

Results and discussion

Artificial neural network architecture

In present study, examples of the different curves of current *versus* time were obtained corresponding to the mixed CC and HQ concentration in spiked compost extract samples. Fig. 1 shows the current response curves for 22 compost extract samples in the training set. The concentrations of CC and HQ in the filtrates both varied from 0.10 to 110 μM. In addition, Fig. 1 presents a maximum and a minimum signal (any of the 38 currents) of the target concentration were included in the training set, avoiding the need for extrapolation when testing

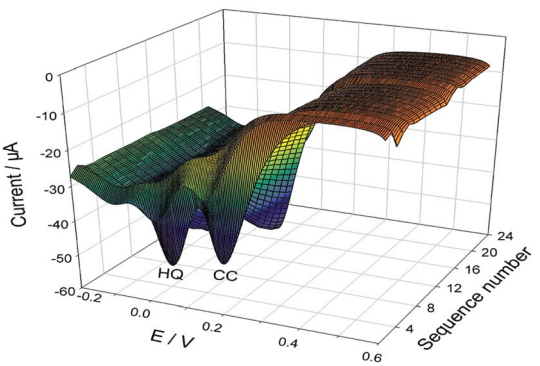

Fig. 1 Measured signals were obtained from 22 compost extract samples using the training set.

the model with the external dataset. It will not give precise results to assign a specific reduction peak potential to each phenolic compound using the statistics of the fitted regression linear model,[12] due to some signal overlapping (as shown in Fig. 1). Therefore, BP-ANN method was used to deconvolve the strong overlapping signal and to quantify the concentrations of two phenolic compounds separately, because ANN modelling was considered to be an appropriate chemometric tool for solving overlapping and nonlinear problems, whose structure was designed to imitate the organization of the human brain.[22]

Generally, a BP-ANN comprises three parts: an input layer, an output layer and in between the two layers, there are one or more hidden layers.[23] Each layer is formed by a series of interconnected neurons, and the value at each neuron is weighted and transformed by a transfer function.[24] A simplified scheme of the procedure followed for the measurement and data processing is shown in Fig. 2. The architecture of the ANN used was defined by these data: the response curves of 22 samples for the training set, the response curves of 8 samples to evaluate model's response, and another 8 extract samples to validate the BP-ANN model application compared with regression liner model. The input layer consisted of a certain number of individual data points of each DPV curve and the output layer consisted of two neurons, namely the two concentrations sought. We used a single intermediate layer, known as the hidden layer, since it was stated that an appropriate level of modelling could be achieved with a single hidden layer in the electrochemical signal resolving process in the relative literature.[25] As we also found in our previous work.[8,26] Thus, Networks with more than one hidden layer were not considered.

Network optimization

A study of the BP-ANN architecture was performed in order to optimize the separate quantifications of the two phenols considered. Twenty-two current intensities at specific potentials for the array of DPV were selected as input vector in the BP-ANN, the corresponding concentrations being the targets that the modelling should reach. The learning accomplished (the degree of modelling) was estimated by the root mean square error (RMSE, eqn (2)). The training process was continued until a preset fitness degree was achieved (RMSE value). Fig. 2 shows the BP-ANN architecture and scheme of this BP-ANN based approach. There are four elements that comprise the ANNs architecture: (a) the number of layers, (b) the number of neurons in each layer, (c) the activation function of each layer, (d) the training algorithm (because this determines the final value of the weights and biases). The number of neurons in each of these two layers is specified by the number of input and output parameters that are used to model each problem so it is readily determined. Therefore, the objective is to find the number of neurons in hidden layer first.[24] Besides, the effects of different transfer function combinations and hidden neuron numbers on the network performance were studied synchronously. Combinations of tan-sigmoidal (Tansig), sat-lineal (Satlin), pure-lineal (Purelin) and log-sigmoidal (Logsig) transfer functions and the hidden neuron numbers (changed from 2 to 16) were tested, as seen on Fig. 3A, with the optimum results of 27 as input neuron number and Levenberg–Marquardt backpropagation (trainlm) as optimization algorithm. Each architecture was retrained five times to get the average RMSEs for the external test set to result in an accurate measure of performance. According to Fig. 3A, the lowest RMSE value was obtained with 10 hidden neurons and Logsig–Purelin as transfer function.

Afterwards, the next step was to determine the importance of network inputs and different optimization algorithms. Similarly, the effects of the input neuron and different optimization algorithms on the model performance were evaluated and optimized in parallel. Fig. 3B shows the RMSEs for different input neuron numbers and optimization algorithms with the optimal transfer function combination of Logsig–Purelin and hidden neuron number of 10. According to Fig. 3B, the BP-

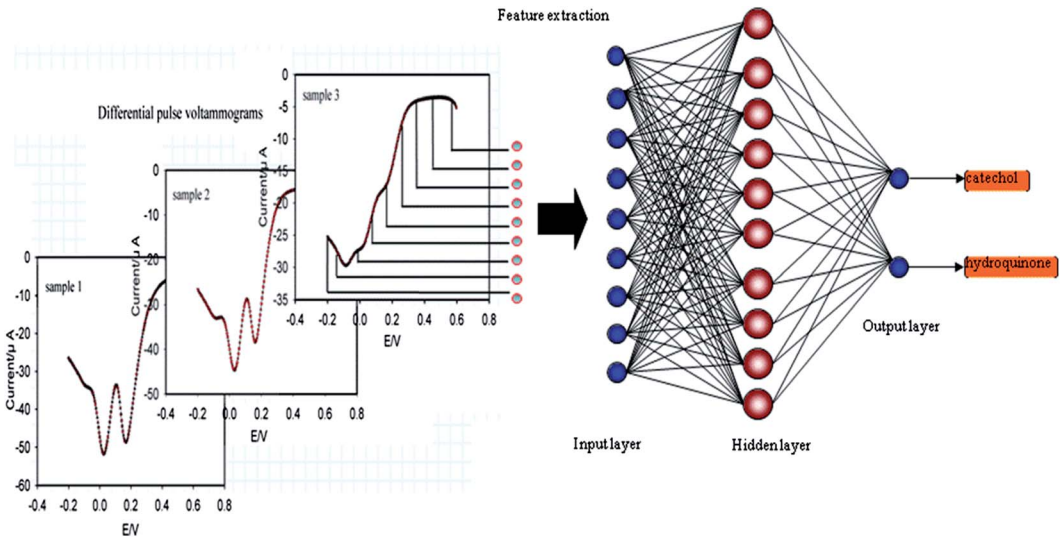

Fig. 2 Example of the ANN architecture used to interpret DPV signals. The input vector comprises 9 to 27 individual data points in the DPV curve. The number of hidden neurons ranges from 2 to 16 (for clarity, only 10 are shown here).

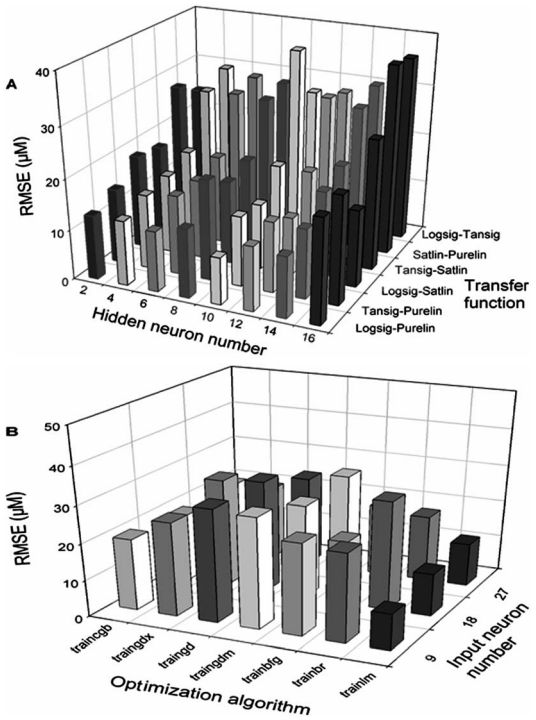

Fig. 3 Obtained RMSEs in: (A) prediction for different transfer function combinations and neuron numbers in the hidden layer with input neuron number of 27 and Levenberg–Marquardt backpropagation (trainlm) as optimization algorithm. (B) Prediction for different input neuron numbers and optimization algorithms with the optimal transfer function combination of Logsig–Purelin and hidden neuron number of 10.

ANN models with trainbr (Bayesian regularization backpropagation), trainbfg (BFGS quasi-Newton method), traingdm (momentum backpropagation), traincgb (Powell–Beale restarts), traingd (gradient descent backpropagation) and traingdx (backpropagation) as optimization algorithms, respectively, could not meet the performance goal and lowest RMSE. So those algorithms were not taken into account. Trainlm (Levenberg–Marquardt backpropagation) was chosen as the one for the best performance. Once the BP-ANN model was trained with inputs that made relatively small contributions to the variance in our experiment, and it was reasonable that the accuracy of the simulation of the ANN model might increase with more input current values, but the training time was prolonged remarkably with no obvious decrease of RMSE. Therefore, the value number of 9 was selected as the input neuron number with adequate accuracy of simulation.

For all these reasons, the best model was obtained by using a $9 \times 10 \times 2$ network that used a Logsig transfer function in the hidden layer and a Purelin function in the output layer with Levenberg–Marquardt backpropagation (trainlm) as optimization algorithm (shown in Table 1).

Performance of the best ANN

Fig. 4 presents the training performances for the two analytes with the optimal BP-ANN configuration, where the predicted concentrations of the two considered phenols were compared with their expected concentrations. The concentrations of CC and HQ added in compost extract in the experiment both varied between 0.10 and 110 μM. Error bars were plotted by five different retrainings with random reinitialization of weights for the best architecture, giving information about the reproducibility of the model. According to Fig. 4, an excellent ability to represent the information on the learning process was obtained with BP-ANN. More valuable was the modelling and prediction capability working with a dataset not included in the learning process. Fig. 5 shows the performance of the best ANN on the external testing subset, with data not included in the learning process. Prediction capability of the model could be considered satisfactory due to the very good correlations obtained in all cases.

Comparison of prediction results between regression model and ANN model in composting system

In order to compare the performance of the BP-ANN model with the linear regression model in respect to correlation coefficient, adaptability to uncertainty, *etc.*, some compost extract samples were spiked with various amounts of the two phenolic compounds distributed in the range of the experimental design. These were prepared and analyzed employing the BP-ANN model and linear regression model. Both the linear model composed of eqn (3) and (4) obtained in our previous work[9] and the BP-ANN model established here was applied to the composting system to predict CC and HQ concentrations in eight compost extract samples.

$$P_{HQ} = -66.954 - 9.5357\log[HQ] \ (P_{HQ}: \mu A, [HQ]: M); \quad (R = 0.9565) \tag{3}$$

$$P_{CC} = -88.394 - 13.081\log[CC] \ (P_{CC}: \mu A, [CC]: M); \quad (R = 0.9771) \tag{4}$$

Practically, there exists a variety of organic compounds in compost extract, such as aromatic, aliphatic, phenolic and quinolic derivatives with varying molecular sizes and properties. It is a complex mixture with diversity, nonlinearity, and uncertain characteristics. In this case, although high specificity and selectivity of biosensor were obtained, when linear model is applied to determine the real samples, the overlapped differential pulse voltammetry signal and the concentration of analyte often exceeds the linear detection range of biosensor, which will affect the accuracy of determination. Therefore, for the sake of obtaining a more applicable and convenient detection method, the combination of biosensors with BP-ANN modelling may turn out to be an alternative tool to classical methods, taking benefit of the advantages of both parts. On one hand, the selectivity, reproducibility and stability of biosensor confirmed the potential applicability for the simultaneous determination of CC and HQ in real environmental samples.[9] On the other hand, the use of ANNs modelling to deconvolve complex signals can enlarge the detection range, and then make the quantification and the result analysis more efficient.[25]

Table 1 Optimal results of ANN architecture and training parameters

Architecture/parameter	Value
Input neuron number	9
Hidden neuron number	10
Output neuron number	2
Transfer function in the hidden layer	Logsig
Transfer function in the output layer	Purelin
Optimization algorithm	Levenberg–Marquardt backpropagation (trainlm)

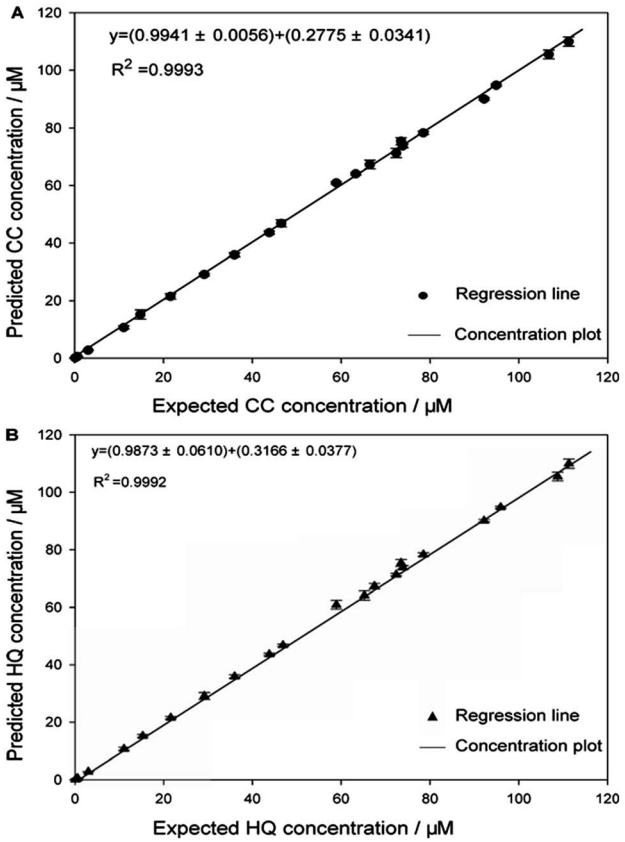

Fig. 4 Modeling performance achieved for the optimized BP-ANN with 22 samples from the training set. Error bars correspond to 5 different retrainings with random reinitialization of weights for the final architecture. Expected concentrations are plotted against those obtained from the BP-ANN, good correlations were obtained for catechol and hydroquinone.

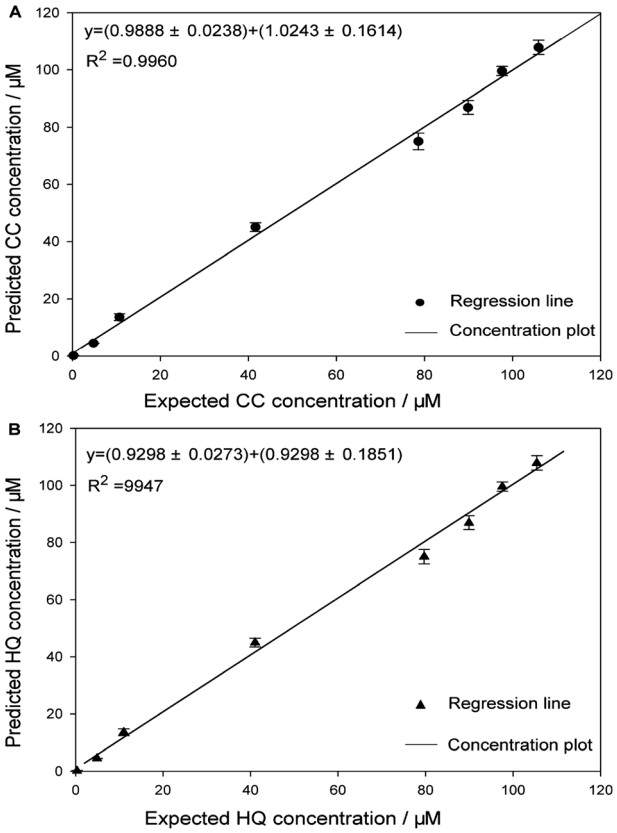

Fig. 5 Modelling performance of the optimised BP-ANN for the external test set. Expected concentrations are plotted against those obtained by BP-AN. Good correlations were obtained for catechol and hydroquinone.

In this study, the DPV peak currents of HQ and CC were linear with correlative concentrations over the range from 4.0×10^{-7} to 8.0×10^{-5} M[9], while the BP-ANN model can directly analyze CC and HQ concentrations varying between 1.0×10^{-7} and 1.1×10^{-4} M. Each calibration was done five times with the relative standard deviations (RSD) not more than 5%. Also in this case, the recovery yield for the two phenolic compounds was calculated, which is summarized in Table 2. As can be seen, the recovery yield of CC obtained by linear regression model ranges from 73.9% to 115.2%, while that obtained by BP-ANN model ranges from 96.0% to 115.3%. It is also observed that the recovery yield of HQ calculated by linear regression model ranges from 74.6% to 119.0%, while that calculated by BP-ANN model ranges from 88.15% to 112.0%. As seen on Table S1,† the RSD in the linear regression model for CC and in the ANN for CC were 7.73% and 3.7781%, respectively. Although the RSD of linear regression model in the compost extract sample of 4 is lower than the RSD of ANN, the RSD of the rest of the samples are lower when analyzed by the ANNs model. In addition, the average (RSD) of ANN is lower than the RSD of linear regression model. What's more, the RSD in the linear regression model for CC (21.2004%) is significantly higher than the RSD for the ANN (2.1151%) when sample concentration exceeded the linear range of the biosensor. Correspondingly, as seen on Table S2,† the RSD in the linear regression model for HQ and in the ANN for HQ were 10.9592% and 4.8468%, respectively. Obviously, the average (RSD) of ANN is lower than the RSD of linear regression model.

The results demonstrated that the prediction results by the ANN model were more precise than the linear regression. The prediction result by linear regression was far from accurate at high levels of CC and HQ beyond the linear range, while the fitting degree of experimental and predicted value using the ANN model were satisfactory (see Table 2), thus confirming the BP-ANN model was superior to the linear

Table 2 Detailed results obtained for the spiked compost extract samples against added concentrations of the two phenolic compounds considered. Recovery yield was also expressed for each compost extract sample

	CC concentration (μM)					HQ concentration (μM)				
Compost extract sample	Added	Predicted[b]	Predicted[a]	Recovery[b]	Recovery[a]	Added	Predicted[b]	Predicted[a]	Recovery[b]	Recovery[a]
1	1.3	1.1 ± 0.37	1.5 ± 0.33	84.6%	115.3%	2.5	2.0 ± 0.46	2.8 ± 0.36	80.0%	112.0%
2	4.6	5.3 ± 0.41	5.0 ± 0.18	115.2%	108.7%	15.5	14.3 ± 0.39	14.9 ± 0.28	92.3%	96.1%
3	17.8	17.4 ± 0.23	17.9 ± 0.11	97.8%	100.6%	20.5	20.0 ± 0.44	20.6 ± 0.37	97.6%	100.5%
4	25.6	27.5 ± 0.44	28.0 ± 0.17	107.4%	109.4%	36.3	31.2 ± 0.40	32.0 ± 0.16	86.0%	88.15%
5	32.3	30.5 ± 0.39	31 ± 0.29	94.4%	96.0%	10.5	12.5 ± 0.29	8.9 ± 0.19	119.0%	88.6%
6	39.5	37.7 ± 0.35	40.3 ± 0.30	95.4%	102.0%	60.5	57.1 ± 0.36	58.6 ± 0.23	94.4%	96.9%
7	59.3	63.5 ± 0.42	60.2 ± 0.15	107.1%	101.5%	83.6	65.8 ± 0.32	85.9 ± 0.29	78.7%	102.8%
8	95.5	70.6 ± 0.47	98.4 ± 0.26	73.9%	103.0%	105.4	78.6 ± 0.38	109.8 ± 0.21	74.6%	104.2%

[a] BP-ANN model. [b] linear model.

regression especially for the determination of high levels of CC and HQ in the compost system. Furthermore, the results also show that the correlation coefficient, adaptability to uncertainty, *etc.*, obtained after combining the biosensor with BP-ANN were superior to direct linear determination of the CC concentration by the biosensor in the compost system. Obviously, combined with the BP-ANN model, the direct detection range for CC and HQ in the compost system of the biosensor were widened, and the satisfactory results confirmed the potential applicability of the biosensor for quantification of CC and HQ in real compost extract sample determination.

Conclusions

In summary, a very good quantification of the two phenolic compounds has been achieved by using the tyrosinase biosensor to get specific signal and BP-ANN as the tool for building the response model. From all the results shown above, it is demonstrated that the combination of tyrosinase biosensor and BP-ANN can give satisfactory quantifications of the CC and HQ concentration simultaneously in composting system with good rapidity and sensitivity. Besides, the direct detection range for CC and HQ of the biosensor was extended to 1.0×10^{-7} to 1.1×10^{-4} M, which was superior to the direct determination by the biosensor with linear data analysis. What is more, this assay provides the potential applicability of the biosensor for the quantification of CC and HQ in composting system though with plenty of interfering substances. In future work, this biosensor combined with artificial neural networks model may be alternatively applied for the quantification of different phenolic mixtures in real contaminated compost samples or other complex environments samples.

Acknowledgements

The study was financially supported by Program for the Outstanding Young Talents of China, the National Natural Science Foundation of China (51222805), the Program for New Century Excellent Talents in University from the Ministry of Education of China (NCET-11-0129), Interdisciplinary Research Project of Hunan University, China Scholarship Council (CSC) (2010843195), the Fundamental Research Funds for the Central Universities, Hunan University, Foundation for the Author of Excellent Doctoral Dissertation of Hunan Province.

References

1 D. Shan, J. Zhang, H. G. Xue, Y. C. Zhang, S. Cosnier and S. N. Ding, *Biosens. Bioelectron.*, 2009, **24**, 3671–3676.
2 L. Lu, L. X. Zhang, S. Zhang, S. Huan, G. Shen and R. Yu, *Anal. Chim. Acta*, 2010, **665**, 146–151.
3 A. Lante, A. Crapisi, A. Krastanov and P. Spettoli, *Process Biochem.*, 2000, **36**, 51–58.
4 S. Canofeni, S. D. Sario, J. Mela and R. Pilloton, *Anal. Lett.*, 1994, **27**, 1659–1662.
5 A. Escarpa, M. D. Morales and M. C. Gonzalez, *Anal. Chim. Acta*, 2002, **460**, 61–72.
6 P. Nagaraja, R. A. Vasantha and K. R. Sunitha, *J. Pharm. Biomed. Anal.*, 2001, **25**, 417–424.
7 B. Levaj, V. D. Uzelac, K. Delonga, K. K. Ganic, M. Banovic and D. B. Kovacevic, *Food Technol. Biotechnol.*, 2010, **48**, 538–547.
8 L. Tang, G. M. Zeng, J. X. Liu, X. M. Xu, Y. Zhang, G. L. Shen, Y. P. Li and C. Liu, *Anal. Bioanal. Chem.*, 2008, **391**, 679–685.
9 T. Lin, Y. Y. Zhou, G. M. Zeng, Z. Li, Y. Y. Liu, Y. Zhang, G. Q. Chen, G. D. Yang, X. X. Lei and M. S. Wu, *Analyst*, 2013, **138**, 3552–3560.
10 F. Despagne and D. L. Massart, *Analyst*, 1998, **123**, 157R–178R.
11 Y. N. Ni and S. Kokot, *Anal. Chim. Acta*, 2008, **626**, 130–146.
12 A. Gutés, F. Céspedes, S. Alegret and M. delValle, *Biosens. Bioelectron.*, 2005, **20**, 1668–1673.
13 X. Cetó, F. Céspedes, M. I. Pividori, J. M. Gutiérrez and M. delValle, *Analyst*, 2012, **137**, 349–356.
14 A. Gutés, A. B. Ibánez, F. Céspedes, S. Alegret and M. delValle, *Anal. Bioanal. Chem.*, 2005, **382**, 471–476.
15 X. Cetóa, J. M. Gutiérrezb, M. Gutiérrezc, F. Céspedesa, J. Capdevilad, S. Mínguezd, C. J. Jorquerac and M. Vallea, *Anal. Chim. Acta*, 2012, **732**, 172–179.
16 X. Ceto, F. Céspedes and M. Valle, *Talanta*, 2012, **99**, 544–551.

17 G. M. Zeng, L. Tang, G. L. Shen, G. H. Huang and C. G. Niu, *Int. J. Environ. Anal. Chem.*, 2004, **84**, 761–774.
18 J. R. M. Smits, W. J. Melssen, L. M. C. Buydens and G. Kateman, *Chemom. Intell. Lab. Syst.*, 1994, **22**, 165–189.
19 I. A. Basheera and M. Hajmeer, *J. Basic Microbiol.*, 2000, **43**, 3–31.
20 M. H. Hassoun, *Fundamentals of Artificial Neural Networks*, MIT Press, Cambridge, MA. 1995.
21 T. Masters, *Practical Neural Network Recipes in C++*, Academic Press, Boston, MA. 1994.
22 F. Rosenblatt, *Psychol. Rev.*, 1958, **65**, 386–408.
23 C. G. Looner, *Pattern Recognition using Neural Networks, Theory and Algorithms for Engineers and Scientists*, Oxford University Press, New York, MA, 1997.
24 P. G. Benardos and G. C. Vosniakos, *Engineering Applications of Artificial Intelligence*, 2007, **20**, 365–382.
25 A. Gutés, A. B. Ibáñez, F. Céspedes, S. Alegret and M. delValle, *Anal. Bioanal. Chem.*, 2005, **382**, 471–476.
26 L. Tang, G. M. Zeng, G. L. Shen, Y. Zhang, G. H. Huang and J. B. Li, *Anal. Chim. Acta*, 2006, **579**, 109–116.

